

Nuclear spin-lattice relaxation rate and nonmagnetic pair-breaking effect in electron-doped $\text{Pr}_{0.91}\text{LaCe}_{0.09}\text{CuO}_{4-y}$: Signature of highly anisotropic s -wave gap

Guo-meng Zhao^{1,2}

¹*Department of Physics and Astronomy, California State University, Los Angeles, CA 90032, USA*

²*Department of Physics, Faculty of Science, Ningbo University, Ningbo, P. R. China*

We numerically calculate the nuclear spin-lattice relaxation rate (R_s) in the superconducting state in terms of anisotropic s -wave gaps. By taking into account electron-phonon coupling, our calculated R_s for a conventional s -wave superconductor, indium, is in quantitative agreement with the experimental data with a clear Hebel-Slichter peak. In contrast, by using the highly anisotropic s -wave gaps inferred from the magnetic penetration depth and scanning tunneling microscopy, our calculated R_s curves for electron-doped $\text{Pr}_{0.91}\text{LaCe}_{0.09}\text{CuO}_{4-y}$ show no Hebel-Slichter peak, in agreement with the experimental data. Finally, the observed weak nonmagnetic pair-breaking effect provides unambiguous evidence for a highly anisotropic s -wave gap in this underdoped cuprate.

The identification of the intrinsic gap symmetry in cuprates is crucial to the understanding of the microscopic pairing mechanism of high-temperature superconductivity, which remains elusive for over twenty years. The superconducting transition temperatures T_c 's of hole-doped cuprates appear to be too high to be explained by the conventional phonon-mediated pairing mechanism. In contrast, the highest T_c in electron-doped (n -type) cuprates is about 40 K, which is within the T_c limit of the conventional phonon-mediated mechanism. Indeed, earlier [1] and recent [2] tunneling spectra in electron-doped cuprates show strong electron-phonon coupling features, similar to the conventional superconductors. The predominantly phonon-mediated pairing should be compatible with an s -wave gap. Many independent experiments designed to test the gap symmetry in the electron-doped system have led to controversial conclusions. Surface-sensitive angle-resolved photoemission spectroscopy (ARPES) [3, 4] implies a d -wave gap with a maximum gap size of about 2.5 meV. This gap size would imply a T_c of about 14 K at the top surface, which is a factor of 1.9 lower than the bulk T_c of 26 K (Ref. [4]). Surface and phase-sensitive experiments [5] provide evidence for pure d -wave order-parameter (OP) symmetry in optimally doped and overdoped n -type cuprates. In contrast, nearly bulk-sensitive point-contact tunneling spectra along the CuO_2 planes [6] show no zero-bias conductance peak (ZBCP) in optimally doped and overdoped samples [7–11], which argues against d -wave gap symmetry. The bulk-sensitive Raman scattering data of $\text{Nd}_{1.85}\text{Ce}_{0.15}\text{CuO}_{4-y}$ imply an anisotropic s -wave gap with a minimum gap Δ_{min} of 3.2 meV (Ref. [12]), which is very close to $\Delta_{min} = 3$ meV inferred from the magnetic penetration depth data [13]. Bulk-sensitive thermal conductivity [14] and specific heat [15] data seem to support d -wave gap symmetry [14, 15] while the same data can be quantitatively explained by nodeless s -wave gap symmetry [16]. The absence of the “Hebel-Slichter” or “coherence” peak below T_c in the nuclear spin-lattice relaxation rate (R_s) of a slightly underdoped n -type $\text{Pr}_{0.91}\text{LaCe}_{0.09}\text{CuO}_{4-y}$ ($T_c = 24$ K) [17]

appears to argue against s -wave gap symmetry. However, the absence of the coherence peak does not necessarily rule out s -wave gap symmetry because there are several mechanisms that can suppress the coherence peak. One of the mechanisms is quasi-particle damping due to strong electron-phonon coupling [18]. Strong electron-electron correlation also leads to a strong suppression of the coherence peak [19]. Furthermore, the coherence peak can be also reduced by gap anisotropy [20, 21]. Therefore, the absence of the coherence peak in the R_s data of $\text{Pr}_{0.91}\text{LaCe}_{0.09}\text{CuO}_{4-y}$ may arise from the combination of the intermediate electron-phonon coupling constant ($\lambda \simeq 1$) [1], strong electron-electron correlation, and a highly anisotropic s -wave gap.

Here we present numerical calculations of the nuclear spin-lattice relaxation rate in the superconducting state in terms of anisotropic s -wave gaps. By taking into account electron-phonon coupling, our calculated R_s for a conventional s -wave superconductor, indium, is in quantitative agreement with the experimental data with a clear Hebel-Slichter peak. In contrast, by using the highly anisotropic s -wave gaps inferred from the magnetic penetration depth and scanning tunneling microscopy, our calculated R_s curves for $\text{Pr}_{0.91}\text{LaCe}_{0.09}\text{CuO}_{4-y}$ show no Hebel-Slichter peak, in agreement with the experimental data. Finally, the observed weak nonmagnetic pair-breaking effect provides unambiguous evidence for a highly anisotropic s -wave gap in this underdoped n -type cuprate.

The expression for the ratio of R_s/R_n of an anisotropic superconductor with a complex gap function is given by [21]

$$\frac{R_s}{R_n} = \frac{2}{k_B T} \int_0^\infty [\langle N(T, \omega) \rangle^2 + \langle M(T, \omega) \rangle^2] f(\omega)[1 - f(\omega)] d\omega, \quad (1)$$

where k_B is the Boltzmann constant, $f(\omega)$ is the Fermi-Dirac distribution function, $\langle N(T, \omega) \rangle$ and $\langle M(T, \omega) \rangle$ are the respective Fermi-surface averages

of $N(T, \omega)$ and $M(T, \omega)$, which are given by

$$N(T, \omega) = \text{Re}\left[\frac{\omega}{\sqrt{\omega^2 - \Delta^2(T, \vec{\Omega})}}\right], \quad (2)$$

and

$$M(T, \omega) = \text{Re}\left[\frac{\Delta(T, \vec{\Omega})}{\sqrt{\omega^2 - \Delta^2(T, \vec{\Omega})}}\right], \quad (3)$$

where $\vec{\Omega}$ is the direction vector on the Fermi-surface. Taking into account electron-phonon coupling, $N(T, \omega)$ and $M(T, \omega)$ can be approximated by [21]

$$N(T, \omega) = \text{Re}\left[\frac{\omega}{\sqrt{\omega^2 - \Delta_1^2(T, \vec{\Omega})(1 + i\delta)^2}}\right], \quad (4)$$

and

$$M(T, \omega) = \text{Re}\left[\frac{\Delta_1(T, \vec{\Omega})(1 + i\delta)}{\sqrt{\omega^2 - \Delta_1^2(T, \vec{\Omega})(1 + i\delta)^2}}\right], \quad (5)$$

where $\Delta_1(T, \vec{\Omega}) = \Delta_0(T)\Delta(\vec{\Omega})$ is the real part of the gap function, $\Delta(\vec{\Omega})$ determines the gap anisotropy, and δ is given by [21]

$$\delta = \frac{n\pi\lambda}{1+\lambda}\left(\frac{T}{\theta_D}\right)^n\left[\Gamma\left(n+\frac{5}{2}\right)\zeta\left(n+\frac{3}{2}\right)\left(\frac{k_B T}{2\Delta_0(T)}\right)^{3/2} + \frac{\sqrt{\pi}}{n}\left(\frac{2\Delta_0(T)}{k_B T}\right)^{3/2}\exp(-\Delta_0(T)/k_B T)\right]. \quad (6)$$

Here Γ and ζ are the Γ and Riemann ζ functions, respectively. At low temperatures, the electron-phonon spectral function $\alpha^2(\omega)F(\omega)$ varies as ω^n . In the following numerical calculations for R_s , we will adopt ‘‘jellium’’ model where $n = 2$ (Ref. [21]).

We first present the results of numerical calculations of R_s for a conventional superconductor, indium. In the calculations, we take the realistic parameters for indium: $\lambda = 0.81$ (Ref. [22]), $\Delta_0(T) = 1.9T_c \tanh[1.81(T_c/T - 1)^{1/2}]$ (Ref. [22]), and $\theta_D = 111$ K (Ref. [23]). We use three simple gap functions to characterize gap anisotropy: $\Delta(\vec{\Omega}) = 1$ for isotropic s -wave gap (s -wave-1); $\Delta(\vec{\Omega}) = (1 - 0.02 \cos 4\phi)$ for a slightly anisotropic s -wave gap (s -wave-2); $\Delta(\vec{\Omega}) = (1 - 0.9 \cos 4\phi)$ for a highly anisotropic s -wave gap (s -wave-3). Fig. 1 shows numerically calculated results of R_s for the three anisotropic s -wave gaps together with the measured R_s for pure indium. It is remarkable that the calculated curve for the isotropic s -wave gap (s -wave-1) is slightly off from the experimental data while the curve for the slightly anisotropic s -wave gap (s -wave-2) almost coincides with the data. In contrast, when the gap becomes highly anisotropic (e.g., s -wave-3), the

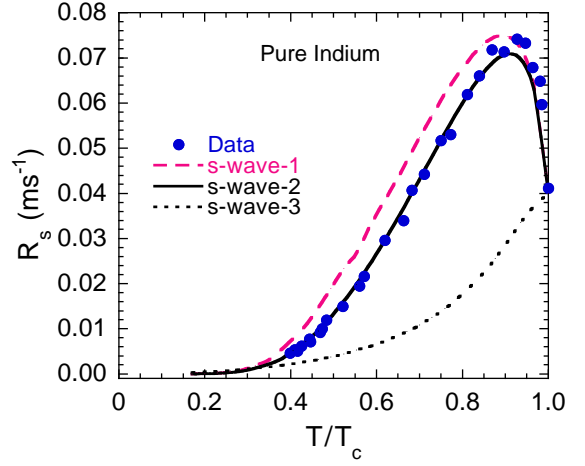


FIG. 1: Nuclear magnetic spin-lattice relaxation rate (R_s) of pure indium (solid circles). The data are taken from Ref. [21]. The numerically calculated R_s for three gap functions: $\Delta(\vec{\Omega}) = 1$ for isotropic s -wave gap (s -wave-1); $\Delta(\vec{\Omega}) = (1 - 0.02 \cos 4\phi)$ for a slightly anisotropic s -wave gap (s -wave-2); $\Delta(\vec{\Omega}) = (1 - 0.9 \cos 4\phi)$ for a highly anisotropic s -wave gap (s -wave-3).

Hebel-Slichter peak is completely removed. This suggests that a highly anisotropic s -wave gap can completely suppress the coherence peak. The numerical results for indium thus provide important insight into how sensitively the coherence peak changes with the gap anisotropy.

In order to address whether the absence of the coherence peak in the R_s data of $\text{Pr}_{0.91}\text{LaCe}_{0.09}\text{CuO}_{4-y}$ can be also explained in terms of a highly anisotropic s -wave gap, we need to extract the gap functions from independent experimental results such as tunneling spectra and the in-plane magnetic penetration depth $\lambda_{ab}(T)$. Fig. 2a shows normalized tunneling conductance of an electron-doped $\text{Pr}_{0.88}\text{LaCe}_{0.12}\text{CuO}_{4-y}$ crystal ($T_c = 24$ K). The normalized tunneling spectrum is reproduced from Ref. [2]. The spectrum was taken on the top CuO_2 plane using scanning tunneling microscopy (STM) [24]. We can numerically calculate the tunneling conductance using the following equation [25]:

$$\frac{dI}{dV} \propto \int_0^{2\pi} p(\theta - \theta_0) \text{Re}\left[\frac{eV - i\Gamma}{\sqrt{(eV - i\Gamma)^2 - \Delta_1^2(\theta)}}\right] d\theta, \quad (7)$$

where θ is the angle measured from the Cu-O bonding direction, Γ is the life-time broadening parameter of an electron, and $p(\theta - \theta_0)$ is the angle dependence of the tunneling probability and equal to $\exp[-\beta \sin^2(\theta - \theta_0)]$. The solid line is the numerically calculated curve using $\Gamma = 0.70$ meV, $\beta = 5.3$, $\theta_0 = \pi/4$, and an anisotropic s -wave gap function: $\Delta_1(0) = 4.9(|1.43 \cos 2\theta - 0.43 \cos 6\theta| + 0.2)$ meV. The finite life-time broadening parameter Γ of an electron may be caused by disorder and inhomogeneities. This life-time broadening effect at zero temperature should be also incorporated into the above expressions for R_s by replacing ω with $\omega - i\Gamma$.

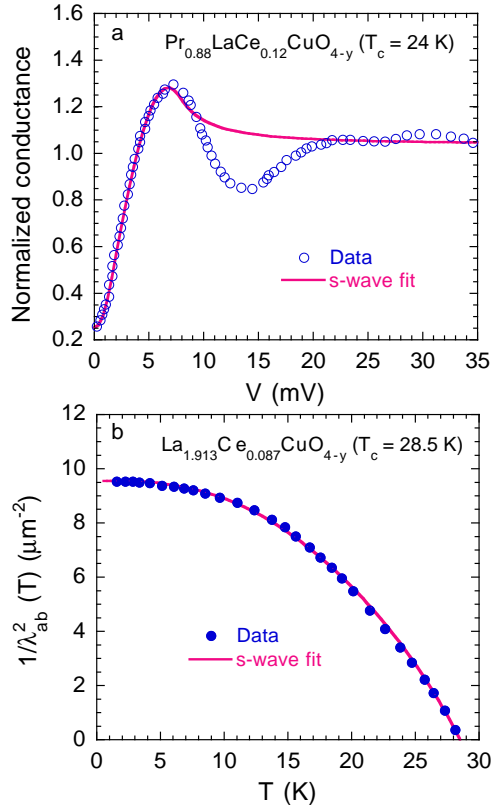


FIG. 2: a) Normalized tunneling conductance of an electron-doped $\text{Pr}_{0.88}\text{LaCe}_{0.12}\text{CuO}_{4-y}$ crystal ($T_c = 24$ K). The solid line is numerically calculated curve using an anisotropic s -wave gap function: $\Delta_1(0) = 4.9(|1.43 \cos 2\theta - 0.43 \cos 6\theta| + 0.2)$ meV. b) Temperature dependence of $1/\lambda_{ab}^2$ for $\text{La}_{1.913}\text{Ce}_{0.087}\text{CuO}_{4-y}$ ($T_c = 28.5$ K). The solid line is the numerically calculated curve using an anisotropic s -wave gap function: $\Delta_1(0) = 3.5(|1.43 \cos 2\theta - 0.43 \cos 6\theta| + 0.35)$ meV.

Figure 2b shows the temperature dependence of $1/\lambda_{ab}^2$ for $\text{La}_{1.913}\text{Ce}_{0.087}\text{CuO}_{4-y}$ ($T_c = 28.5$ K), which has a similar doping level as $\text{Pr}_{0.91}\text{LaCe}_{0.09}\text{CuO}_{4-y}$. The data are digitized from Ref. [26]. We can numerically calculate the temperature dependence of $\lambda_{ab}^2(0)/\lambda_{ab}^2(T)$ for an anisotropic gap function using the following equation: [27]

$$\frac{\lambda_{ab}^2(0)}{\lambda_{ab}^2(T)} = 1 + (1/\pi) \int_0^{2\pi} \int_0^\infty d\theta d\epsilon \frac{\partial f}{\partial E}. \quad (8)$$

Here $E = \sqrt{\epsilon^2 + \Delta_1^2(\theta, T)}$. The solid line is the numerically calculated curve using an anisotropic s -wave gap function: $\Delta_1(T, \theta) = 3.5 \tanh[1.81(T_c/T - 1)^{1/2}](|1.43 \cos 2\theta - 0.43 \cos 6\theta| + 0.35)$ meV. If we assume that the superconducting gap is proportional to T_c , then the bulk superconducting gap of $\text{Pr}_{0.91}\text{LaCe}_{0.09}\text{CuO}_{4-y}$ inferred from the penetration depth data is $2.95(|1.43 \cos 2\theta - 0.43 \cos 6\theta| + 0.35)$ meV.

Now we can use the inferred gap functions from both STM and magnetic penetration depth to calculate R_s for $\text{Pr}_{0.91}\text{LaCe}_{0.09}\text{CuO}_{4-y}$. In the calculations, we take the realistic parameters for the electron-doped cuprate: $\lambda = 1.0$ (Ref. [1]) and $\theta_D = 384$ K (Ref. [15]). Since the R_s data were taken in a magnetic field of 6.2 T which suppresses T_c to about 20 K, we scale down the gap size proportional to T_c . For the gap function extracted from the tunneling spectrum, the same life-time broadening parameter ($\Gamma = 0.7$ meV) in the tunneling spectrum is used to calculate R_s . This parameter only influences R_s at low temperatures and has little effect on R_s close to T_c .

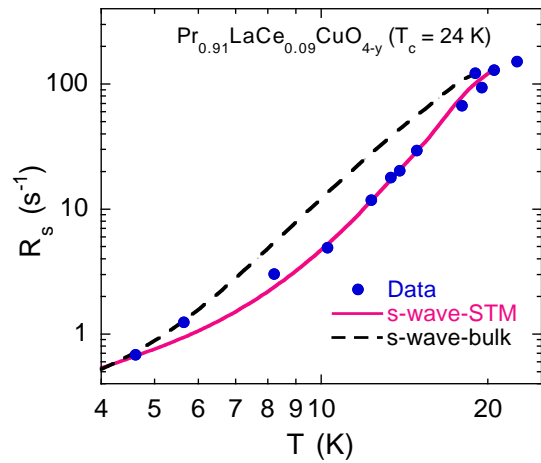


FIG. 3: Nuclear magnetic spin-lattice relaxation rate (R_s) in $\text{Pr}_{0.91}\text{LaCe}_{0.09}\text{CuO}_{4-y}$ (solid circles). The solid and dashed lines are the numerically calculated R_s curves for the s -wave gap functions inferred from STM (denoted as STM) and from the magnetic penetration depth (denoted as bulk).

The calculated results are shown in Fig. 3. It is apparent that for the gap function extracted from STM, the calculated R_s curve (solid line) agrees excellently with the experimental data. On the other hand, for the bulk gap function, the calculated curve (dashed line) deviates significantly from the data. In all the cases, the coherence peaks are absent. Therefore, the absence of the coherence peak in the R_s data could be consistent with highly anisotropic s -wave gaps.

Although the R_s data can be excellently explained in terms of the gap function inferred from STM, it does not necessarily imply that the gap function deduced from STM is more realistic than that inferred from the magnetic penetration depth. As a matter of fact, the above calculations do not take into account strong electron-electron correlation. It was shown that strong electron-electron correlation can reduce the coherence peak of R_s for an s -wave gap and cause R_s to drop more rapidly just below T_c [19]. For the slightly underdoped $\text{Pr}_{0.91}\text{LaCe}_{0.09}\text{CuO}_{4-y}$, the measured value of $T_1TK_s^2$ (where T_1 is the spin-lattice relaxation time and K_s is the spin part of Knight shift) is a factor of 50 smaller than the expected value of noninteracting elec-

trons [17]. This implies strong electron-electron correlation. Therefore, it is very likely that the R_s data can be quantitatively explained in terms of the bulk anisotropic s -wave gap if the strong electron-electron correlation is taken into account.

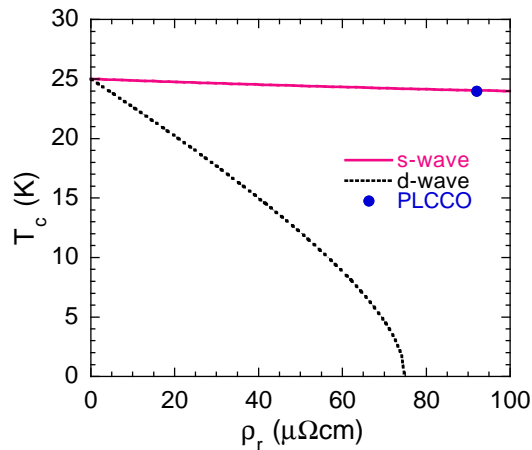


FIG. 4: The calculated curve of T_c versus residual resistivity in terms of any d -wave gap (dotted line) and the bulk anisotropic gap (solid line): $\Delta = 2.95(|1.43 \cos 2\theta - 0.43 \cos 6\theta| + 0.35)$ meV. In the calculations, we use $\hbar\Omega_p^* = 0.62$ eV. The solid circle is a data point for $\text{Pr}_{0.91}\text{LaCe}_{0.09}\text{CuO}_{4-y}$ (PLCCO) [17].

In order to unambiguously distinguish between any d -wave and anisotropic s -wave gap symmetries, we study the response of a superconductor to nonmagnetic impurities or disorder. The nonmagnetic impurity pair-breaking effect is both bulk- and phase-sensitive. This is because the rate of T_c suppression by nonmagnetic impurities [28] is determined by the value of the Fermi surface (FS) average $\langle \Delta(\vec{k}) \rangle_{FS}$, which depends sensitively on the phase of the gap function. More specifically, the rate is proportional to a parameter $\chi = 1 - (\langle \Delta(\vec{k}) \rangle_{FS})^2 / \langle \Delta^2(\vec{k}) \rangle_{FS}$. It is easy to show that $\chi = 1$ for any d -wave gap and $\chi = 0.058$ for the highly anisotropic s -wave gap: $\Delta = 2.95(|1.43 \cos 2\theta - 0.43 \cos 6\theta| + 0.35)$ meV. An equation to describe the pair-breaking effect by nonmagnetic impurities (or defects) is given by [28]

$$\ln \frac{T_{c0}}{T_c} = \chi \left[\Psi\left(\frac{1}{2} + \frac{0.122(\hbar\Omega_p^*)^2 \rho_r}{T_c}\right) - \Psi\left(\frac{1}{2}\right) \right], \quad (9)$$

where $\hbar\Omega_p^*$ is the renormalized plasma energy [28, 29] in units of eV, ρ_r is the residual resistivity in units of $\mu\Omega\text{cm}$, and Ψ is the digamma function. The lower limit of $\hbar\Omega_p^*$ is equal to $\hbar\Omega_s^*$ which is related to the zero-temperature penetration depth $\lambda_{ab}(0)$. For $\text{La}_{1.913}\text{Ce}_{0.087}\text{CuO}_{4-y}$, $\lambda_{ab}(0) = 320$ nm (Ref. [26]), leading to $\hbar\Omega_s^* = 0.62$ eV. Figure 4 shows the calculated curves of T_c versus residual resistivity in terms of any d -wave gap (dotted line) and the bulk anisotropic s -wave gap (solid line): $\Delta = 2.95(|1.43 \cos 2\theta - 0.43 \cos 6\theta| + 0.35)$ meV. For the d -wave gap, T_c is suppressed to 0 at $\rho_r = 74.6 \mu\Omega\text{cm}$ when the lower limit of $\hbar\Omega_p^* = 0.62$ eV is used. In

$\text{Pr}_{1.85}\text{Ce}_{0.15}\text{CuO}_{4-y}$ ($T_c = 20$ K), $\hbar\Omega_p^*$ is found to be a factor of 1.65 larger than $\hbar\Omega_s^*$ due to a finite mean-free path [30]. If we increase $\hbar\Omega_p^*$ of $\text{Pr}_{0.91}\text{LaCe}_{0.09}\text{CuO}_{4-y}$ by the same factor (1.65), T_c will be suppressed to 0 at $\rho_r = 27.4 \mu\Omega\text{cm}$ for the d -wave gap. The measured large ρ_r of $92 \mu\Omega\text{cm}$ and nearly optimal T_c of 24 K in $\text{Pr}_{0.91}\text{LaCe}_{0.09}\text{CuO}_{4-y}$ rules out any d -wave gap symmetry.

In summary, the absence of the Hebel-Slichter peak in the nuclear spin-lattice relaxation rate of $\text{Pr}_{0.91}\text{LaCe}_{0.09}\text{CuO}_{4-y}$ can be well explained by a highly anisotropic s -wave gaps inferred respectively from the magnetic penetration depth and scanning tunneling microscopy. The observed weak nonmagnetic pair-breaking effect provides unambiguous evidence for a highly anisotropic s -wave gap in this slightly underdoped n -type cuprate.

-
- [1] Q. Huang *et al.*, Nature (London) **347**, 369 (1990).
 - [2] G. M. Zhao, Phys. Rev. Lett. **103**, 236403 (2009).
 - [3] N. P. Armitage *et al.*, Phys. Rev. Lett. **86**, 1126 (2001).
 - [4] H. Matsui *et al.*, Phys. Rev. Lett. **95**, 017003 (2005).
 - [5] C. C. Tsuei, and J. R. Kirtley, Phys. Rev. Lett. **85**, 182 (2000); A. D. Darminto *et al.*, Phys. Rev. Lett. **94**, 167001 (2005).
 - [6] Ya. G. Ponomarev *et al.*, Physica C **243**, 167 (1995).
 - [7] S. Kashiwaya *et al.*, Phys. Rev. B **57**, 8680, (1998).
 - [8] Amlan Biswas *et al.*, Phys. Rev. Lett. **88**, 207004 (2002).
 - [9] M. M. Qazilbash *et al.*, Phys. Rev. B **68**, 024502 (2003).
 - [10] L. Shan *et al.*, Phys. Rev. B **72**, 144506 (2005).
 - [11] L. Shan *et al.*, Phys. Rev. B **77**, 014526 (2008).
 - [12] G. M. Zhao, cond-mat/arXiv: 0907.2011.
 - [13] L. Alff *et al.*, Phys. Rev. Lett. **83**, 2644 (1999).
 - [14] N.P. Armitage, P. Fournier, and R. L. Greene, cond-mat/arXiv: 0906.2931.
 - [15] Hamza Balci and R. L. Greene, Phys. Rev. Lett. **93**, 067001 (2004).
 - [16] G. M. Zhao, cond-mat/arXiv: 0909.1009.
 - [17] G. Q. Zheng *et al.*, Phys. Rev. Lett. **90**, 197005 (2003).
 - [18] P.B. Allen and D. Rainer, Nature (London) **349**, 396 (1991).
 - [19] N. Bulut and D. J. Scalapino, Phys. Rev. B **45**, 2371 (1992).
 - [20] L. C. Hebel, Phys. Rev. **116**, 79 (1959).
 - [21] J. D. Williamson and D. E. MacLaughlin, Phys. Rev. B **8**, 125 (1973), and references therein.
 - [22] J. P. Carbotte, Rev. Mod. Phys. **62**, 1027 (1990).
 - [23] B. S. Chandrasekhar and J. A. Rayne, Phys. Rev. **124**, 1011 (1961).
 - [24] F. C. Niestemski *et al.*, Nature (London) **450**, 1058 (2007).
 - [25] K. Suzuki *et al.*, Phys. Rev. Lett. **83**, 616 (1999).
 - [26] John A. Skinta *et al.*, Phys. Rev. Lett. **88**, 207005 (2002).
 - [27] T. Jacobs *et al.*, Phys. Rev. Lett. **75**, 4516 (1995).
 - [28] L. A. Openov, Phys. Rev. B **58**, 9468 (1998).
 - [29] R. J. Radtke, K. Levin, H.-B. Schutter, M. R. Norman, Phys. Rev. B **48**, 653 (1993).
 - [30] C. C. Homes *et al.*, Phys. Rev. B **74**, 214515 (2006).